PHYSICAL REVIEW C **79**, 051601(R) (2009)

Suppression of complete fusion in the ^{6}Li + ^{144}Sm reaction

P. K. Rath,[1] S. Santra,[2,*] N. L. Singh,[1] R. Tripathi,[3] V. V. Parkar,[2] B. K. Nayak,[2] K. Mahata,[2] R. Palit,[4] Suresh Kumar,[4] S. Mukherjee,[1] S. Appannababu,[1] and R. K. Choudhury[2]

[1]*Department of Physics, M. S. University of Baroda, Vadodara-390002, India*

[2]*Nuclear Physics Division, Bhabha Atomic Research Centre, Mumbai-400085, India*

[3]*Radiochemistry Division, Bhabha Atomic Research Centre, Mumbai-400085, India*

[4]*Department of Nuclear and Atomic Physics, Tata Institute of Fundamental Research, Mumbai-400005, India*

(Received 11 November 2008; revised manuscript received 31 March 2009; published 11 May 2009)

Complete fusion excitation function for the ^{6}Li + ^{144}Sm reaction has been measured at near barrier energies by the activation technique. Coupled-channel calculations show an enhancement in fusion cross section at energies below the barrier compared to the one-dimensional barrier penetration model calculation, but they overpredict it in the entire energy range compared to the experimental data. Reduced fusion cross sections for the present system at energies normalized to the Coulomb barrier were also found to be systematically lower than those with strongly bound projectiles forming a similar compound nucleus. These two observations conclusively show that the complete fusion cross section, at above barrier energies, is suppressed by ∼32% in the ^{6}Li + ^{144}Sm reaction. Reanalyses of existing fusion data for ^{7}Li + ^{165}Ho and ^{7}Li + ^{159}Tb also show a suppression compared to those with strongly bound projectiles, which contradicts earlier conclusions. The fusion suppression factor seems to exhibit a systematic behavior with respect to the breakup threshold of the projectile and the atomic number of the target nucleus.

DOI: 10.1103/PhysRevC.79.051601 PACS number(s): 25.70.Jj, 25.70.De, 25.70.Mn

The effect of the breakup of weakly bound (stable or radioactive) nuclei on the fusion process is a subject of current experimental and theoretical interest [1,2]. Although subbarrier fusion involving strongly bound stable nuclei is well understood, there are contradictory results and predictions about the enhancement or suppression of the fusion cross section $\sigma_{\rm fus}$, over predictions of the single fusion barrier, around the Coulomb barrier, when one of the collision partners is a weakly bound nucleus. Experimental investigations of the fusion process have been made with stable weakly bound ^{6,7}Li [3,4] and ^{9}Be [5,6] nuclei; however, they have different conclusions about fusion enhancement/suppression, when compared with strongly bound stable isotopes [7] and/or coupled-channel calculations [8,9]. There are theoretical calculations that predict either suppression of the complete fusion (CF) cross sections [10,11] due to breakup of loosely bound nucleus or enhancement [12,13] of the same due to coupling of the relative motion of the colliding nuclei to the breakup channel.

Hagino *et al.* [14] performed an improved coupled-channel calculation that predicts the enhancement of fusion at subbarrier energies and reduction at above barrier energies. An understanding of breakup and fusion is directly relevant to producing nuclei near the drip line and possibly superheavy nuclei. Experimentally such studies are limited because of the low intensities of unstable beams currently available. Light nuclei such as ^{6}Li, which breaks up into $\alpha + d$ with a breakup threshold of only 1.48 MeV, has a large breakup probability. Fusion with such a nucleus is ideal for the quantitative testing of theoretical models and for use as a comparator for fusion measurements with other unstable beams.

In this paper, we present precise excitation function measurements for the complete fusion of ^{6}Li with ^{144}Sm, by activation method, at energies ranging from 20 to 40 MeV in steps of 2 MeV, i.e., 0.75 to 1.5 times the Coulomb barrier ($V_B^{\rm lab} \approx$ 26.2 MeV). The target nucleus ^{144}Sm ($Z = 62$, $N = 82$) was chosen because it is a spherical nucleus, which minimizes the target effect on fusion, and that makes the effect of projectile breakup more evident. Coupled-channel calculations to find the influence of breakup on fusion are presented. The present data have been compared with those involving strongly bound projectiles (^{12}C + ^{141}Pr and ^{20}Ne + ^{133}Cs) forming similar compound nuclei. The existing data from the literature [3,15,16] for two more systems (^{7}Li + ^{165}Ho and ^{7}Li + ^{159}Tb) involving loosely bound projectiles have also been reanalyzed to look for any systematic behavior on the suppression of fusion cross sections.

The present experiment was performed at the 14UD BARC-TIFR Pelletron facility, Mumbai, using a ^{6}Li beam incident on ^{144}Sm (94% enriched) targets having thicknesses in the range of 450–678 μg/cm^2. These targets were prepared by electrodeposition on an Al backing of thickness 2.2 mg/cm^2. The thickness of the targets was measured by the Rutherford backscattering method using a 60 MeV ^{16}O beam. For the fusion measurement, the target was mounted with an additional Al backing downstream. The thickness of the Al backing was sufficient to completely stop all the evaporation residues (ERs) produced during irradiation. According to the half-life of the ERs that were expected to be formed in significant abundance, each of the 11 targets was irradiated for 4–5 h by the ^{6}Li beam with energy $E_{\rm lab}$ = 20–40 MeV, in steps of 2 MeV. The beam current was ∼60 nA, and the beam flux

*ssantra@barc.gov.in

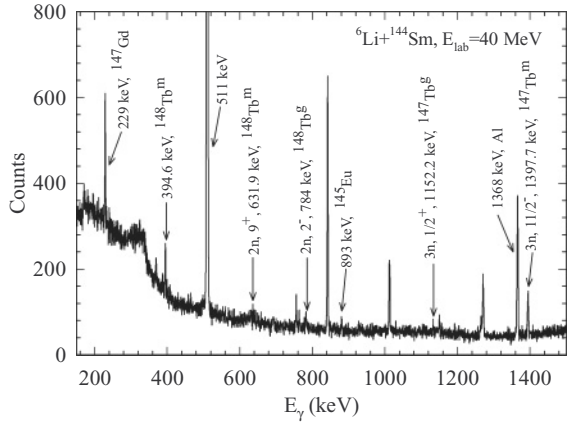

FIG. 1. Typical γ-ray spectra showing γ lines of different ERs populated via CF in the ^{6}Li + ^{144}Sm system at projectile energy $E_{\rm lab} = 40$ MeV.

was calculated by the total charge collected in the Faraday cup placed behind the target using a precision current integrator device. The reaction products, which were stopped in the target and Al backing, were identified by their characteristic γ rays by off-line counting using a high-purity Ge detector coupled to a multichannel analyzer. A ^{152}Eu source was used for the energy calibration as well as for the efficiency measurement. The standard γ source and the irradiated samples were counted in the same geometry. Figure 1 shows a typical off-line γ-ray spectrum for beam energy $E_{\rm lab} = 40$ MeV, where different ERs populated via CF in the ^{6}Li + ^{144}Sm system are identified. The dominant decay channels were observed to be $2n$ and $3n$ evaporation. Corresponding nuclear data, such as half-lives $T_{1/2}$, γ-ray energies E_{γ}, and branching ratios I_{γ}, etc., are given in Table I. The intense γ lines were chosen to evaluate the cross sections.

After $2n$ evaporation of the compound nucleus, the residue nucleus ^{148}Tb can be populated either in the ground state (g.s.) or the metastable state (m.s.) and then decay into ^{148}Gd by electron capture with half-lives of 60 min and 2.2 min, respectively. Similarly for $3n$ evaporation, ^{147}Tb decays to ^{147}Gd with half-lives of 1.7 h (g.s.) and 1.83 min (m.s.). Intensities of the γ lines with proper branching ratios corresponding to both ground and metastable states of ^{148}Tb(^{147}Tb) together give the cross sections of the $2n(3n)$ channel. The excitation function for individual ER channels are shown in Figs. 2(a) and 2(b).

To obtain the relative contribution of other residue channels, statistical model (SM) calculations were performed using

TABLE I. Observed evaporation residues corresponding to CF in the ^{6}Li + ^{144}Sm reaction for ground (g) and metastable (m) states, and their decay data.

Reactions	ER	E_{γ} (keV)	$T_{1/2}$	J^{π}	I_{γ} (%)
^{144}Sm(^{6}Li, $3n$)	^{147}Tb^{m}	1397.7 (m)	1.83 min	$11/2^{-}$	83.2
^{144}Sm(^{6}Li, $3n$)	^{147}Tb^{g}	1152.2 (g)	1.65 h	$1/2^{+}$	72.5
^{144}Sm(^{6}Li, $2n$)	^{148}Tb^{m}	631.9 (m)	2.2 min	9^{+}	95
^{144}Sm(^{6}Li, $2n$)	^{148}Tb^{g}	784(g)	1.0 h	2^{-}	100

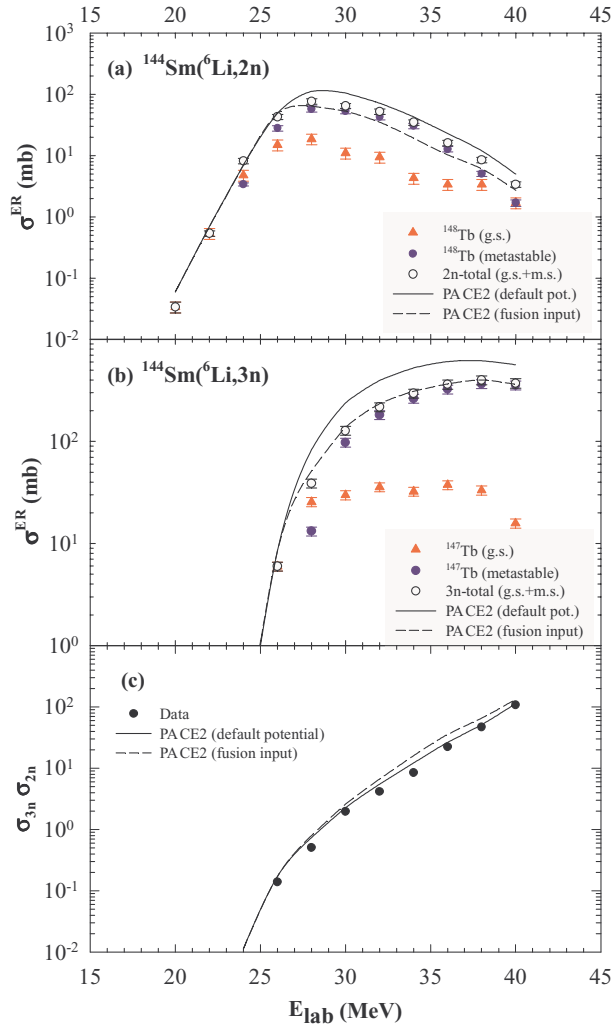

FIG. 2. (Color online) ER cross sections for ground state (filled triangles) and metastable state (filled circles) of (a) ^{148}Tb nucleus at different $E_{\rm lab}$. Total ER (g.s. + m.s.) for the $2n$ channel are represented by open circles. (b) Same as (a), but for the ^{147}Tb nucleus, i.e, $3n$ ER channel. (c) Ratio of σ_{3n} to σ_{2n} (see text for details).

the code PACE2 [17] with default potential parameters. For energies below the Coulomb barrier, the SM calculations were carried out by feeding the ℓ distribution obtained from external coupled-channel calculations. The results of PACE2 calculations for the ratio of σ_{3n} to σ_{2n} with level density ρ equal to $A/10$ (solid line) are shown in Fig. 2(c), which provide a good description of the present experimental data. The value of σ_{3n}/σ_{2n} was found to be less sensitive to the level density parameter (for $\rho = A/10$, $A/9$, and $A/8$). Calculated cross sections for $2n$ and $3n$ channels are plotted as solid lines in Figs. 2(a) and 2(b). The ratio, $R_{\sigma}^{\rm theory}(= \frac{\sigma_{2n}+\sigma_{3n}}{\sigma_F})$, of the combined cross section of the $2n$ and $3n$ channels $(\sigma_{2n} + \sigma_{3n})$ to the complete fusion (σ_F) was calculated at each energy using the same parameters in PACE2. As can be seen from Table II, the combined cross sections of $2n$ and $3n$ are dominant (~92–56%) in the entire energy range (20–40 MeV) of our measurement. The complete fusion $\sigma_{\rm fus}^{\rm expt}$ was determined by dividing the cumulative cross sections of

TABLE II. Experimental cross sections for $2n$-ER, $3n$-ER, and total fusion with R_σ^{theory} from PACE2 calculations.

E_{lab} (MeV)	$\sigma_{2n}^{\text{expt}} + \sigma_{3n}^{\text{expt}}$ (mb)	R_σ^{theory}	$\sigma_{\text{fus}}^{\text{expt}}$ (mb)
20	0.034 ± 0.01	0.8571	0.04 ± 0.01
22	0.54 ± 0.06	0.9211	0.59 ± 0.08
24	8.2 ± 0.8	0.8979	9.13 ± 1.10
26	49 ± 4.9	0.8302	59.0 ± 6.0
28	116 ± 12	0.8263	140 ± 15
30	192 ± 12	0.8152	236 ± 15
32	270 ± 13	0.8055	335 ± 18
34	331 ± 16	0.7933	417 ± 27
36	378 ± 19	0.7530	502 ± 30
38	407 ± 21	0.6709	607 ± 31
40	374 ± 20	0.5551	674 ± 33

two measured channels ($2n$ and $3n$) by the ratio R_σ^{theory} as shown in Table II.

Further, to check the consistency in SM results for different channels, $\sigma_{\text{fus}}^{\text{expt}}$ was given as input to PACE2 and its output for σ_{2n}, σ_{3n} and their ratio are plotted as dashed lines in Fig. 2, which are found to be reasonably close to the data. The errors in $\sigma_{\text{fus}}^{\text{expt}}$ include the errors in ERs as well as the uncertainty in the SM calculations.

The measured excitation function for complete fusion and the corresponding barrier distribution are shown in Fig. 3. The distribution of fusion barriers $D(B)$ was calculated by $d^2(\sigma_{\text{fus}} E_{\text{c.m.}})/dE_{\text{c.m.}}^2$ using the measured σ_{fus} and then normalized, so as to get $\int D(B)\,dB = 1$, which is shown in Fig. 3(b). Coupled-channel calculations using the CCFULL code [18] are performed with the potential parameters that reproduce the average fusion barrier ($V_B = 25.1 \pm 0.3$ MeV) of the experimental $D(B)$. The value of V_B was obtained following the procedure adopted in Ref. [7]. Parameters for the Akyuz-Winther (AW) potential and modified potential used for coupled-channel (CC) calculations, and the corresponding uncoupled barrier heights V_B and radii R_B and curvatures $\hbar\omega$, derived for the present system as well as several other systems, are given in Table III. The projectile ground state (1^+) with spectroscopic quadrupole moment, $Q = -0.082$ fm^2, and the unbound first excited state (3^+, 2.186 MeV) are coupled. A

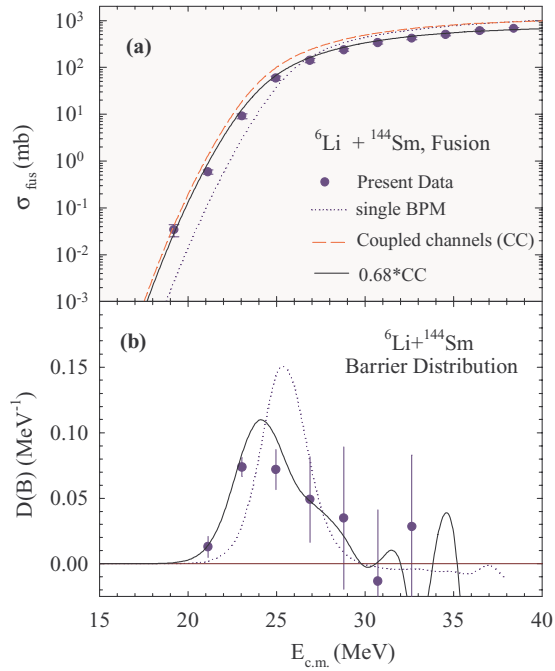

FIG. 3. (Color online) (a) Complete fusion cross section (filled circles) and (b) corresponding normalized barrier distribution (filled circles) for $^6\text{Li} + ^{144}\text{Sm}$ compared with coupled (dashed lines) and uncoupled (dotted lines) results from CCFULL [18] calculations. Solid lines are obtained by multiplying the coupled results by a factor of 0.68.

value of $B(E2; 1^+ \rightarrow 3^+) = 21.8\ e^2\,\text{fm}^4$ is used for the 3^+ rotational excitation (same as in Ref. [4]). The target excitation state (3^-, 1.81 MeV) is coupled as a vibrational state. Coupling of the breakup channel is not considered. The results of the coupled-channel calculations are shown in Fig. 3. It can be seen from Fig. 3(a) that at energies below the barrier, there is a large enhancement of fusion cross section with coupling (dashed line) compared to the uncoupled values (dotted lines). But, the coupled results overpredict the measured fusion data over the entire energy range. However, it was interesting to see that the measured fusion cross section agrees very well with the calculated ones when multiplied by a factor of 0.68 (solid line) over the entire energy range. This implies that there is

TABLE III. Parameters for AW and CC potential, along with V_B, R_B, and $\hbar\omega$.

System	Potential	V_0 (MeV)	r_0 (fm)	a (fm)	V_B (MeV)	R_B (fm)	$\hbar\omega$ (MeV)
$^6\text{Li} + ^{144}\text{Sm}$	AW	42.33	1.158	0.63	24.65	10.2	4.85
	CC	47.00	1.100	0.63	25.55	9.78	5.04
$^{12}\text{C} + ^{141}\text{Pr}$	AW	54.71	1.177	0.63	45.07	10.6	4.55
$^{20}\text{Ne} + ^{133}\text{Cs}$	AW	63.40	1.187	0.63	68.20	10.9	4.33
$^7\text{Li} + ^{165}\text{Ho}$	AW	45.61	1.160	0.63	25.44	10.7	4.50
	CC	170.00	0.950	0.95	23.78	11.12	3.50
$^{12}\text{C} + ^{160}\text{Gd}$	AW	55.38	1.180	0.63	47.75	10.9	4.61
$^7\text{Li} + ^{159}\text{Tb}$	AW	45.48	1.165	0.63	24.84	10.6	4.45
	CC	132.00	0.980	0.85	24.17	10.68	3.81
$^4\text{He} + ^{162}\text{Dy}$	AW	35.18	1.470	0.63	17.48	10.2	4.11

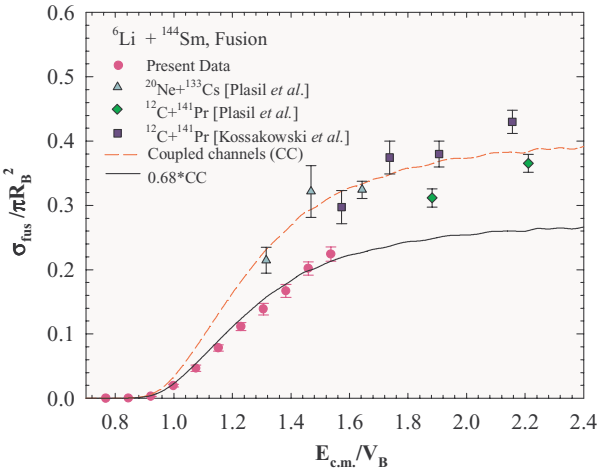

FIG. 4. (Color online) Reduced cross sections ($\sigma_{\rm fus}/\pi R_B^2$) as a function of $E_{\rm c.m.}/{\rm V}_B$ for the present system (filled circles) along with two other reactions ^{12}C + ^{141}Pr (filled diamonds [19], filled squares [20]) and ^{20}Ne + ^{133}Cs (filled triangles [20]). Dashed line is the result of coupled-channel calculation. Solid line is obtained by multiplying the coupled results by a factor of 0.68.

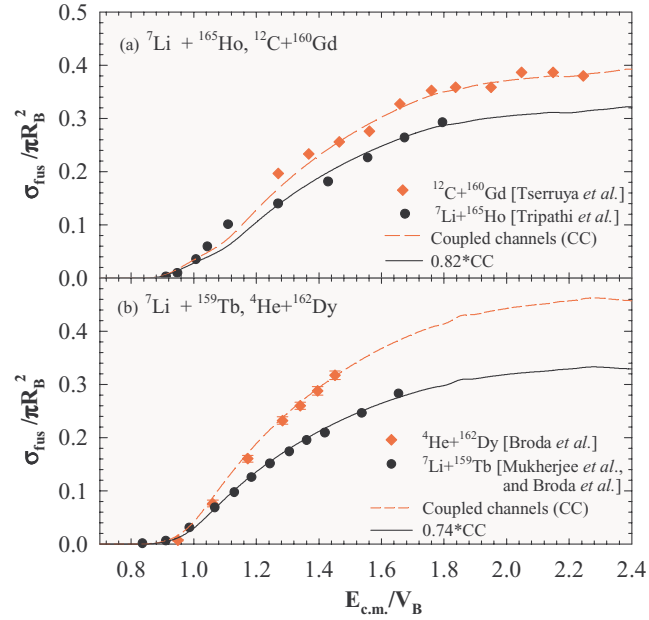

FIG. 5. (Color online) Reduced cross sections ($\sigma_{\rm fus}/\pi R_B^2$) as a function of $E_{\rm c.m}/{\rm V}_B$ for (a) ^{7}Li + ^{165}Ho (filled circles [3]) along with ^{12}C + ^{160}Gd (filled diamonds [21]) and (b) ^{7}Li + ^{159}Tb (filled circles [16]) along with ^{4}He + ^{161}Dy (filled diamonds [15]). Dashed lines are the result of coupled-channel calculation. Solid lines are obtained by multiplying the coupled results by a factor of (a) 0.82 and (b) 0.74.

an overall suppression of ∼32% of the fusion cross section in the entire energy range compared to the ones predicted by CCFULL. An uncertainty of ±5% in suppression factor is estimated from the uncertainties in V_B and σ_F. The normalized barrier distribution obtained from the calculated fusion cross sections [Fig. 3(b)] shows that the experimental $D(B)$ agrees reasonably well with the coupled (solid line) one, which is very different from the uncoupled (dotted line) distribution.

To see the effect of the breakup of loosely bound projectile ^{6}Li on fusion cross sections, the present data were compared with the data for other systems forming similar compound nuclei but involving strongly bound projectiles [19,20]. Figure 4 shows the comparison of the reduced cross sections ($\sigma_{\rm fus}/\pi R_B^2$) as a function of $E_{\rm c.m.}/{\rm V}_B$ for the present system along with two other systems ^{12}C + ^{141}Pr [19,20] and ^{20}Ne + ^{133}Cs [20] forming the compound nucleus ^{153}Tb. It is interesting to see that the reduced fusion cross sections involving strongly bound projectiles (^{12}C + ^{141}Pr and ^{20}Ne + ^{133}Cs) are much larger than those for the present system, and they agree very well with the results of coupled-channel calculations using CCFULL without any suppression factor. This confirms that the complete fusion for ^{6}Li + ^{144}Sm is suppressed by 32 ± 5% compared to those with the stable projectiles as well as those predicted by the fusion model adopted in CCFULL. Any model dependence on calculated fusion at subbarrier energies, where couplings are important, can be singled out by having more fusion data for the systems involving tightly bound projectiles. The suppression in fusion cross section may be a direct consequence of the loss of incident flux due to the projectile breakup, which seems to be independent of energy over the measured energy range.

The above observation on fusion suppression is quite different from what Tripathi *et al.* [3] concluded for ^{7}Li + ^{165}Ho, ^{7}Li + ^{159}Tb [15], and ^{9}Be + ^{208}Pb [5] systems. To find whether their conclusions remain valid, the data for ^{7}Li + ^{165}Ho and ^{7}Li + ^{159}Tb [15,16] were reanalyzed in the same line as above. The advantages and/or differences in the present analysis compared with the earlier one are (i) comparison of the fusion data with a system involving tightly bound projectile forming the same compound nucleus, (ii) use of an improved version of the coupled-channel code to take care of nonlinear couplings of all orders, and (iii) comparison of fusion data with coupled results (instead of uncoupled ones) to estimate the suppression. The reduced fusion cross sections for the above two systems have been compared with those of ^{12}C + ^{160}Gd [21] and ^{4}He + ^{162}Dy [15], respectively, forming the same compound nuclei, as shown in Fig. 5. The parameters for the potential barrier used in CC calculations for these systems are given in Table III. CC potentials are chosen to reproduce the average fusion barrier of the barrier distribution derived from the fusion data. For ^{7}Li + ^{165}Ho, the effect of deformation was calculated by coupling to the ground state rotational band (with $\beta_2 = 0.285$ and $\beta_4 = 0.024$, $E_x = 0.077$ MeV) of the deformed target nucleus, following the method of Ref. [16]. Projectile deformation could not be included, as CCFULL cannot handle both the deformed target and deformed projectile. For the pair transfer coupling, the channel ^{165}Ho(^{7}Li, ^{4}He), with a positive Q value of 10.5 MeV, whose cross section was measured to be maximum [3], was included. A form factor of 0.85 was used, which reproduces the fusion data well. Coupling parameters of CCFULL calculations for ^{7}Li + ^{159}Tb were same as those of Ref. [16]. It is interesting to find that the fusion for ^{7}Li-induced reactions is suppressed by about 18% and 26%, respectively, compared to those involving strongly bound projectiles of ^{12}C

TABLE IV. Fusion suppression factor for different systems.

Projectile	Breakup threshold (MeV)	Target	Suppression factor	Ref.
^{6}Li	$S_{\alpha d} = 1.48$	^{209}Bi	36%	[7]
^{6}Li	$S_{\alpha d} = 1.48$	^{208}Pb	34%	[22]
^{6}Li	$S_{\alpha d} = 1.48$	^{144}Sm	32%	Present data
^{9}Be	$S_{\alpha\alpha n} = 1.57$	^{208}Pb	32%	[23]
^{9}Be	$S_{\alpha\alpha n} = 1.57$	^{144}Sm	10%	[24]
^{7}Li	$S_{\alpha t} = 2.45$	^{209}Bi	26%	[7]
^{7}Li	$S_{\alpha t} = 2.45$	^{165}Ho	18%	[3], Re-analysis
^{7}Li	$S_{\alpha t} = 2.45$	^{159}Tb	26%	[16]

or ^{4}He forming the same compound nuclei. These results are quite different from the conclusions drawn in Ref. [3].

Similar suppression in complete fusion cross sections has been observed in several other reactions involving loosely bound nuclei but forming different compound nuclei. The results are summarized in Table IV. It is observed that the suppression has a clear dependence on two main factors, i.e., (i) breakup threshold of the projectile and (ii) charge of the target nucleus. For a particular projectile, the suppression increases with the increase in the Z of the target. Similarly, for a particular target, the suppression increases with a decrease in the breakup threshold. Thus, it indicates that the reduction in the complete fusion cross section is mainly due to the breakup of the projectile in the Coulomb field of the target nucleus.

In summary, the complete fusion excitation function for the ^{6}Li + ^{144}Sm reaction has been measured at energies near and above the Coulomb barrier. An activation technique was used to determine the cross sections of $2n$ and $3n$ evaporation channels, which were the most dominating channels of decay of the compound nucleus formed by the complete fusion process in the measured energy range. Statistical model calculations were performed using PACE2 to estimate the relative contributions of other residue channels in order to determine the experimental cross sections for the complete fusion. Coupled-channel calculations using CCFULL show an enhancement in fusion at energies below the barrier compared to the predictions given by the single barrier penetration model. However, the experimental results suggest that there is an overall suppression of the fusion cross section, particularly at energies above the barrier, for the present reaction as compared to CCFULL calculations with full couplings. A comparison of the results for the present system with other systems involving strongly bound stable projectiles such as ^{12}C + ^{141}Pr and ^{20}Ne + ^{133}Cs forming similar compound nuclei, clearly shows that fusion cross sections for the present system are systematically lower. From these two comparisons, fusion suppression was estimated to be 32 ± 5%. This suppression may be ascribed to the low breakup threshold energy of ^{6}Li, which allows it to break up prior to fusion.

A similar procedure was applied to reanalyze the fusion data from the literature for ^{7}Li + ^{165}Ho and ^{7}Li + ^{159}Tb, and it was found that the cross sections are suppressed by about 18% and 26% compared to those with ^{12}C + ^{160}Gd [21] and ^{4}He + ^{162}Dy [15] systems, respectively, forming the same compound nuclei. Most importantly, these results are different from the earlier conclusions of Tripathi *et al.* [3].

A systematic comparison of fusion excitation functions for several reactions involving loosely bound stable projectiles shows that the suppression in fusion is a common phenomenon, and it increases with (i) the increase in the target atomic number Z_T and (ii) the decrease of the projectile breakup threshold E_{th}. To obtain an empirical expression for the suppression as a function of Z_T and E_{th}, the fusion data for a large number of reactions involving loosely bound projectiles is necessary.

The authors would like to thank the Pelletron crew for the smooth operation of the accelerator during the experiments. P.K.R acknowledges the financial support of BRNS (No. 2007/37/7), India, in carrying out these investigations.

[1] L. F. Canto, P. R. S. Gomes, R. Donangelo, and M. S. Hussein, Phys. Rep. **424**, 1 (2006).
[2] N. Keeley, R. Raabe, N. Alamanos, and J. L. Sida, Prog. Part. Nucl. Phys. **59**, 579 (2007).
[3] V. Tripathi *et al.*, Phys. Rev. Lett. **88**, 172701 (2002).
[4] C. Beck *et al.*, Phys. Rev. C **67**, 054602 (2003).
[5] M. Dasgupta *et al.*, Phys. Rev. Lett. **82**, 1395 (1999).
[6] I. Padron *et al.*, Phys. Rev. C **66**, 044608 (2002).
[7] M. Dasgupta *et al.*, Phys. Rev. C **70**, 024606 (2004).
[8] A. Diaz-Torres and I. J. Thompson, Phys. Rev. C **65**, 024606 (2002).
[9] A. Diaz-Torres, I. J. Thompson, and C. Beck, Phys. Rev. C **68**, 044607 (2003).
[10] M. S. Hussein, M. P. Pato, L. F. Canto, and R. Donangelo, Phys. Rev. C **46**, 377 (1992).
[11] N. Takigawa, M. Kuratani, and H. Sagawa, Phys. Rev. C **47**, R2470 (1993).
[12] C. H. Dasso *et al.*, Nucl. Phys. **A405**, 381 (1983).
[13] M. Dasgupta *et al.*, Annu. Rev. Nucl. Part. Sci. **48**, 401 (1998).
[14] K. Hagino, A. Vitturi, C. H. Dasso, and S. M. Lenzi, Phys. Rev. C **61**, 037602 (2000).
[15] R. Broda *et al.*, Nucl. Phys. **A248**, 356 (1975).
[16] A. Mukherjee *et al.*, Phys. Lett. **B636**, 91 (2006).
[17] A. Gavron, Phys. Rev. C **21**, 230 (1980).
[18] K. Hagino *et al.*, Comput. Phys. Commun. **123**, 143 (1999).
[19] F. Plasil *et al.*, Phys. Rev. Lett. **45**, 333 (1980).
[20] R. Kossakowski *et al.*, Phys. Rev. C **32**, 1612 (1985).
[21] I. Tserruya *et al.*, Phys. Rev. Lett. **60**, 14 (1988).
[22] Y. W. Wu *et al.*, Phys. Rev. C **68**, 044605 (2003).
[23] D. J. Hinde *et al.*, Phys. Rev. Lett. **89**, 272701 (2002).
[24] P. R. S. Gomes *et al.*, Phys. Rev. C **73**, 064606 (2006).